Classification: Biological Sciences / Physiology

When two cells are better than one: specialized stellate cells provide a privileged route for uniquely rapid water flux in *Drosophila* renal tubule

Pablo Cabrero[a], Selim Terhzaz[a], Anthony J. Dornan[a], Saurav Ghimire[a], Heather L. Holmes[b,c], Daniel R. Turin[b,d], Michael F. Romero[b,c], Shireen A. Davies[a] and Julian A. T. Dow[a]

[a]Institute of Molecular, Cell and Systems Biology, College of Medical, Veterinary and Life Sciences, University of Glasgow, Glasgow G12 8QQ, UK

[b]Department of Physiology and Biomedical Engineering and [c]Division of Nephrology and Hypertension, Mayo Clinic College of Medicine & Science, Rochester, MN 55905;
[d]University of Minnesota Rochester, Rochester, MN 55905

Author for correspondence: julian.dow@glasgow.ac.uk

Running title: Aquaporins mediate unique fluid flux rates

Keywords: Malpighian tubule, *Drosophila melanogaster*, aquaporin, *Xenopus* oocyte, stellate cell

Abstract

Insects are highly successful, in part through an excellent ability to osmoregulate. The renal (Malpighian) tubules can secrete fluid faster on a per-cell basis than any other epithelium, but the route for these remarkable water fluxes has not been established. In *Drosophila melanogaster*, we show that 4 members of the Major Intrinsic Protein family are expressed at very high level in the fly renal tissue; the aquaporins Drip and Prip, and the aquaglyceroporins Eglp2 and Eglp4. As predicted from their structure and by their transport function by expressing these proteins in *Xenopus* oocytes, Drip, Prip and Eglp2 show significant and specific water permeability, whereas Eglp2 and Eglp4 show very high permeability to glycerol and urea. Knockdowns of any of these genes impacts tubule performance resulting in impaired hormone-induced fluid secretion. The *Drosophila* tubule has two main secretory cell types: active cation-transporting principal cells with the aquaglyceroporins localize to opposite plasma membranes and small stellate cells, the site of the chloride shunt conductance, with these aquaporins localising to opposite plasma membranes. This suggests a model in which cations are pumped by the principal cells, causing chloride to follow through the stellate cells in order to balance the charge. As a consequence, osmotically obliged water follows through the stellate cells. Consistent with this model, fluorescently labelled dextran, an *in vivo* marker of membrane water permeability, is trapped in the basal infoldings of the stellate cells after kinin diuretic peptide stimulation, confirming that these cells provide the major route for transepithelial water flux. The spatial segregation of these components of epithelial water transport may help to explain the unique success of the higher insects.

Significance statement

The tiny insect renal (Malpighian) tubule can transport fluid at unparalleled speed, suggesting unique specialisations. Here we show that strategic allocation of Major Intrinsic Proteins (MIPs) to specific cells within the polarized tubule allow the separation of metabolically intense active cation transport from chloride and water conductance. This body plan is general to at least many higher insects, providing a clue to the unique success of the class Insecta.

Introduction

There are more species of insects than all other forms of life combined. In part, this is because of the exceptional ability of the simple body plan to operate in a wide range of environments, and osmoregulation is a key component of this success. Remarkably, the insect Malpighian (renal) tubule is capable of secreting fluid faster (on a per cell volume basis) than any other epithelium known (1, 2). In *Drosophila*, the renal tubule has two major cell types (3-5); the mitochondria-rich principal cell

actively transports protons via an apical, plasma membrane V-ATPase (6), setting up a gradient which is exchanged primarily for potassium (7, 8) and enters the cell basolaterally through a combination of Na^+, K^+-ATPase (9), potassium channels (10, 11) and cotransports (12-14). The smaller stellate cell (15, 16) provides a route for hormone-stimulated (17-20) chloride conductance through a basolateral ClC-a chloride channel (21), and secCl, an apical cys-loop chloride channel (22), to balance the lumen-positive charge, and so effect a net movement of salt. Aquaporins (e.g., the water transporting MIP proteins) are known to be highly expressed in insect tubules (23-27), and global knockdown of an aquaporin in the *Aedes* mosquito (28-30), or in the beetle *Tribolium* (31) impacts water loss. However, the route or mechanism of the very high osmotically-obliged water fluxes that produce such remarkable fluid output has not been characterised. Here, using the powerful cell-specific transgenic technologies unique to *Drosophila melanogaster* (32), we show that this flux is transcellular, and selectively through the stellate cells, mediated by two aquaporins, in response to diuretic hormone stimulation.

Results & Discussion

Tubules express 4 members of the Major Intrinsic Protein family

Major intrinsic proteins (MIPs) are a multigene family of 6-transmembrane domain proteins, that assemble as tetramers to form pores (33). Most members of the family are true water channels (aquaporins); others can facilitate movement of water or small organic molecules (aquaglyceroporins); and the substrates of some are still obscure (33). In *Drosophila*, eight genes make up the MIP family (**Fig. 1**), but the FlyAtlas and FlyAtlas2 gene expression online resources (25, 34, 35) independently report that only four are expressed at high levels in epithelia such as the salivary gland, midgut, hindgut and Malpighian tubules (**Fig. 1**). Two of these highly expressed genes (*Drip* and *Prip*) are similar to classical aquaporins in structure, whereas the other two (*Eglp2* and *Eglp4*) align with the aquaglyceroporins (36). Comparison of the protein sequence of *Drosophila melanogaster* aquaporins (Drip and Prip) and aquaglyceroprins (Eglp2 and Eglp4) in a Clustal Omega alignment shows that key active-site residues, including those required for water selectivity and those involved for their regulation, have been conserved (**Fig. S1**). There are thus at least two candidates that could mediate high water flux rates in polarized epithelia.

Each MIP localises to a different membrane domain within the tubule

Water and solutes transport are achieved by an apicobasally polarized distribution of membrane proteins, and accordingly, it is important to establish where in the tubule principal and stellate cells MIPs reside. We raised specific antibody against the four tubule-expressed MIPs and validated them by Western blotting (**Fig. S2 and Fig. S3**). Immunocytochemistry showed clear segregation of MIPs

expression, with the two aquaporins expressed on opposite sides of the specialized stellate cell (Drip and Prip are localised to the basolateral and apical membranes respectively, **Fig. 2 *A* and *B***), and the two aquaglyceroporins on opposite sides of the main principal cell (Eglp2 and Eglp4 are localised to the basolateral and apical membranes respectively, **Fig. 2 *C* and *D***). Accordingly, overexpression of all 4 MIPs label with Venus (eYFP) recapitulate the pattern of expression observed by immunocytochemistry (**Fig. 2 *A'-D'***). These data are consistent with other reports that Drip and Prip show spatial separation in other insects, such as silkworm (37). It would thus be tempting to surmise that the stellate cell provides a major route for water flux through the tissue; but only the transport properties of one of these MIPs (Drip) has been established (23); how many of them are in fact functional aquaporins?

Stellate cell MIPs are aquaporins; Principal cell MIPs are aquaglyceroporins

Each of the four candidate genes was expressed in *Xenopus* oocytes, and tested both for classical swelling under hypoosmotic stress, and for facilitated flux of organic solutes. The two channels expressed in tubules (Drip and Prip) both acted as classical aquaporins, showing rapid water fluxes, but only barely detectable fluxes of organic solutes (**Fig. 3 *A* and *B***). By contrast, the Eglp2 and Eglp4 channels showed more modest fluxes of water, but rapid fluxes of small organic solutes, such as glycerol and urea, consistent with their predicted classification as aquaglyceroporins {Drake, 2015 #8090}. These data are thus in agreement with Drip and Prip providing a transcellular route for water through the stellate cells, and as the tubule provides a range of physiological readouts, this prediction can be tested experimentally.

Knockdown of AQPs reduces fluid transport and impacts survival

Although epithelial polarisation of some AQPs has been shown in other insects (23, 26, 37, 38), *Drosophila* genetic technology allows their physiological roles to be dissected with great precision. Using the GAL4/UAS system and renal cell-type specific drivers, it is possible to generate transgenic flies in which a single candidate gene is knocked down in only the tubule cell type in which it is expressed, leaving expression throughout the rest of the fly untouched. Accordingly, each of the four genes was knocked down in the cell-type in which their proteins had been shown to be expressed, and we were able to confirm by qPCR and immunocytochemistry the efficiency of the knockdown of MIPs expression at the gene and protein levels (**Fig. 4 *A* and 2 *A'-D'***). The resulting fluid output was then measured under baseline conditions, and when maximally stimulated with diuretic peptides of the capa and kinin families. Knockdown of either *Drip* or *Prip* in just the stellate cell significantly impeded fluid secretion, confirming functional roles in rapid fluid movement across the tissue (**Fig. 4 *B***). However, knockdown of *Eglp2* or *Eglp4* in the principal cells also elicited reduced fluid secretion

rates (**Fig. 4 *B***). This suggested two possibilities; either that all four MIPs could produce water conductance, through both cell types (at variance with the biophysical characterisation, **Fig. 3**), or that one pair of channels provided the main route for water, while the other pair allowed flux of an organic osmolyte, or metabolic substrate, such that blockade could reduce overall function of the tissue.

The very high rates of generation of primary urine by the tubule could become a liability under dry conditions, and so knockdown of aquaporins would be predicted to impact survival under desiccation. This was shown by global knockdown of the *Drip* orthologue in *Anopheles gambiae*, the malaria vector (26); however, *Drip* is broadly expressed, and so the effect could not be attributed to the tubules (28, 29). Using GAL4/UAS technology, we were able to knock down *Drip* or *Prip* expression in just the tubule stellate cells, and show that this was sufficient to produce enhanced survival under desiccation stress (**Fig. S4**). Water flux across the tubule is thus limiting for terrestrial insects under desiccation stress, as previously suggested (39).

The route of water flux is through the stellate cells

To distinguish the roles of the aquaglyceroporins from the aquaporins, it would be necessary to determine the route of water flux through the tubule. The complex polyglucan, dextran, can be readily fluorescently labelled, and also can be size-selected to ranges that can be swept along by water flux, but then trapped in a pathway of restricted permeability. Both the principal and stellate cells have apical microvilli, which in principal cells are stabilised by Fas2 (40) and contain mitochondria to support intense activity of the V-ATPase (41); and both cell types also possess basal infoldings, that increase the available surface area for transport (42). We thus stimulated tubules in the presence of fluorescently-labelled dextran, which pilot experiments had shown was too large to move across the epithelium. Dextran would thus accumulate in a compartment diagnostic of the route of water movement, be it the principal or stellate cells, or the paracellular route between the tight ('septate') junctions (43). The results showed that only the basal labyrinths of the stellate cells became labelled with 40 kDa dextran (**Fig. 5 *A* and *C***), and that the percentage of stellate cell population displaying uptake of dextran was significantly higher after kinin stimulation (**Fig. 5 *C***), thereby implying that the pathway provided by Prip and Drip in the stellate cells is the major route for water movement through the tubule.

Generality of the stellate cell model

The segregation of active cation transport to principal cells, and chloride and water flux to stellate cells, may confer selective advantages and could potentially extend to other insects. Stellate cells are more widely distributed than previously thought (15); and we have previously shown that

fluorescently-labelled kinin (the neuropeptide that stimulates the chloride conductance (4, 18)) marks stellate-like cells in most advanced endopterygote insects (44), suggesting an ancient and conserved role. To probe the route of water flux in insects without the benefits of *Drosophila* transgenics, we applied the dextran flux labelling technique to a panel of insects selected to represent the major exo- and endopterygote Orders, so providing an initial view on the two cell model (**Fig. 6**). Among the exopterygote insects, dextran selectively labelled stellate-like cells of all insect Orders except the beetles, where an extensive network was observed. Significantly, kinin genes are almost never found in this Order (45), consistent with a lack of cell specialisation. In the more primitive exopterygotes, the story is more varied; although kinin had labelled the epithelium rather generally, this general pattern was seen in the locust, but not a cockroach. As a first approximation, therefore, the two-cell model, that links chloride flux, kinin stimulation and water flux, seems to have broad applicability across the higher insect; but further sampling of multiple species will be required.

A revised model for a high-flux epithelium

The tubule shows a remarkable ability to secrete primary urine at very high rates; and together with other recent results, it is becoming clear that this success relies on the functional segregation of transport between different cell types (**Fig. 7**). The main, principal cell has long apical microvilli (40), each containing a mitochondrion (41), and loaded with proton-pumping V-ATPase and is thought to drive an exchanger from the NHA family to produce a net K^+ flux. Basolaterally, the infoldings contain high levels of Na^+, K^+-ATPase (46), inward rectifier K^+ channels (10, 11), and $Na^+/K^+/Cl^-$ cotransporters (14). This metabolically active cell is likely the route for excretion of a wide range of solutes via ABC transporters and other organic solute transporters, many of which hare abundantly expressed in the tubule (24). The rarer stellate cells, by contrast have shorter microvilli and fewer mitochondria, but are the gatekeepers for the hormone-stimulated chloride shunt conductance (through basolateral ClC-a and apical secCl), and also for the passage of osmotically obliged water through basolateral Prip and apical Drip aquaporins. The metabolically active principal cell is thus sheltered from these very high, and potentially disruptive, fluxes of water.

Given the severe consequences of unregulated fluid loss to a small terrestrial insect, it is not surprising that the tubule is under sophisticated neurohormonal control (47). Whereas cation pumping by the principal cells is under control of DH31 (48), DH44 (49) and Capa (50) neuropeptides, the stellate cells are independently controlled by the neuropeptide kinin (19, 51) and by the biogenic amine tyramine (17); both act indistinguishably through intracellular calcium (17, 52). The chloride shunt conductance is a known target of kinin and tyramine, as both rapidly collapse the lumen-positive potential (17, 18); however, it will be interesting to investigate whether one or both of this

messengers have an independent action to regulate stellate cell aquaporins, perhaps through phosphorylation or recruitment to the plasma membrane.

This two-cell model is likely to be widely applicably through the higher insects, the endopterygotes, which include flies, butterflies and bees, in which a secondary cell type has been observed either directly (15), or by mapping an aquaporin (26), or by visualisation with fluorescently labelled kinin (the hormone which regulates chloride flux) (44), or by otherwise mapping the kinin receptor (53, 54). However, a universal model is unlikely, as most members of one higher insect Order (the Coleoptera) do not use kinin signalling (44); and in the lower exopterygote insects, such as crickets, there is no evidence for specialised secondary cells. The next challenge will be to map out the generality of this two-cell model, and its alternatives, across the tens of millions of species that makes up the insects.

Materials & Methods

Informatics

The MIP amino acid sequences were obtained from *Drosophila* gene database Flybase (flybase.org) and multiple sequence alignment was performed using Clustal Omega (www.ebi.ac.uk/Tools/msa/clustalo). Phosphorylation sites were analysed using GPS 3.0 algorithm (gps.biocuckoo).

Drosophila Stocks and Rearing

Flies were reared at 22°C, 45% relative humidity on a 12:12 photoperiod on standard *Drosophila* media. The following lines (with original source) for this study were: Wild-type *D. melanogaster Canton-S* (Bloomington stock #1); *c724*-GAL4 (3) and *ClC-a*-GAL4 (VDRC #202625) driver lines specific to stellate cells, and used interchangeably in this study; *CapaR*-GAL4 driver line specific to principal cells (55, 56); *UAS-Drip-Venus* (21); dsRNA line directed against *Eglp2/CG17664* (VDRC #101847); *Eglp4/CG4019* (NiG-Fly stock #4019R-2); *Prip/CG7777* and *Drip/CG9023* respectively (NiG-Fly stock #7777R-2 and #9023R-2).

Generation of Transformants

UAS-Prip-Venus, *UAS-Eglp2-Venus* and *UAS-Eglp4-Venus* were generated by PCR amplifying the coding sequence of the respective *Drosophila* MIP genes using DreamTaq green PCR master mix (Thermo Fisher Scientific) and the primer pairs listed in **Table S1**. ORF amplicons were cloned into pENTR donor vector (Invitrogen) and transferred to pTWV destination vector (DGRC) using Gateway® LR Clonase® II Enzyme mix according to manufacturing instructions (Thermo Fisher Scientific).

Sequences integrity were confirmed by GATC Biotech and transgenic lines were generated by using standard methods for P-element mediated germ-line transformation (BestGene).

Quantitative RT-PCR

For validation of tubule mRNA expression, qRT-PCR was performed using an ABI StepOnePlus Detection System (Applied Biosystems) with Brilliant III Ultra-Fast SYBR Green QPCR master mix (Agilent, UK) and the primer pairs listed in **Table S1**. Data were normalized against the *rpl32* standard and expressed as fold change compared to controls ± SEM (n = 3).

Antibody Production and Immunohistochemistry

Antigenic peptides were identified using Abdesigner software (57). Rabbit anti-peptide antibodies were raised against the Drip epitope (CFKVRKGDDETDSYDF), Prip epitope (CNEASEKYRTHADERE), Eglp2 epitope (CSEVDETTMSTKRTSE), and Eglp4 epitope (CTSNEKLRQLEDVQLS) by Genosphere Biotechnologies (Paris, France).

Malpighian tubules from 7-day old flies were dissected in Schneider's medium (Thermo Fisher Scientific) and transfer to poly-L-lysine (Sigma-Aldrich)-covered 35-mm glass-bottomed dishes (MatTek Corporation) in PBS, fixed in 4% (w/v) paraformaldehyde in PBS for 30 min at room temperature, washed in PBT (PBS + 0.05% (v/v) Triton X-100), and then blocked in 10% (v/v) normal goat serum (Sigma-Aldrich) in PBT. IgG purified rabbit anti-Drip/Prip/Eglp2/Eglp4 peptides (dilution 1:1000) were used. Alexa Fluor 488/564-conjugated affinity-purified goat anti-rabbit antibodies (Thermo Fisher Scientific) were used at a concentration of 1:1000 for visualisation of the primary antiserum. Incubations in the primary and secondary antibodies were performed overnight at 4°C. Tubules were incubated with the nuclear stain DAPI (1 µg mL^{-1}; Sigma-Aldrich) for 1 min and in some cases Rhodamine/Alexa-633 coupled phalloidin (1:100; Thermo Fisher Scientific) in PBT for a minimum of 30 min. Samples were washed repeatedly in PBS before being mounted in Vectashield (Vector Laboratories Inc). Confocal images were taken using an LSM 880 inverted microscope (Zeiss) and processed with Zen black/blue software (Zeiss, Oberkochen, Germany) and Adobe Photoshop/Illustrator CS 5.1.

Western Blotting

For each fly line, Malpighian tubules from >50 flies were dissected under Schneider's *Drosophila* medium (Thermo Fisher Scientific) and were transferred to 100 µl RIPA buffer (150 mM NaCl, 10 mM Tris-HCl pH 7.5, 1 mM EDTA, 1% Triton X-100, 0.1% (wt/v) SDS) with 1 µl of protease inhibitor cocktail (Sigma-Aldrich). Samples were homogenized using a Microson XL2000 sonicator (Misonix Inc. NY, USA), and centrifuged (13,000 rpm) at 4°C for 10 min. Protein concentrations were measured using the Bradford Protein Assay (Bio-Rad Technologies). Approximately 20 µg protein

from each sample was electrophoresed on a NuPage 4–12% Bis-Tris gel and blotted onto nitrocellulose membrane using the Novex system (Thermo Fisher Scientific). Blots were stained with Ponceau S and probed with IgG purified rabbit anti-Drip/Prip/Eglp2/Eglp4 antibodies (1 µg mL^{-1}) and developed by electrochemiluminescence assay using ECL™ horseradish peroxidase linked anti-rabbit IgG (1:2000; Amersham Biosciences).

Fluid Secretion

Secretion assays were performed as described previously (2). Malpighian tubules from 7-day-old adult female flies were dissected under Schneider's insect medium (Thermo Fisher Scientific) and isolated into 10 µl drops of a 1:1 mixture of Schneider's medium : *Drosophila* saline. Intact tubules were left to secrete for approximately 30 min before starting the experiment. Secretion rates were measured every 10 min; after 30 min of baseline readings, the diuretic peptide *Drosophila* kinin (DK) and capa-1 were added to 10^{-7}M, and secretion rates measured for a further 30 min. Data are plotted as mean ± SEM (n > 7).

Dextran Labelling

Individuals were lightly anaesthetised using either $C0_2$ or ice and their Malpighian tubules dissected in Schneider's *Drosophila* medium (Thermo Fisher Scientific). Dissected tissues were then pre-incubated for 10-20 min at room temperature in a solution of 1:1 Schneider's:PBS with neuropeptides (e.g. Kinin, DH31, DH44) present at a concentration of 10^{-7} M (stimulated) or with no neuropeptides (non-stimulated). The dissected tissues were then transferred to fresh Schneider's:PBS solution containing 0.2% dextrans (40 kDa or 70 kDa; Thermo Fisher Scientific) conjugated to a specified fluor, for 2 – 5 min at room temperature. Tissues were fixed for 10 min in 2% (w/v) paraformaldehyde, stained with 1 µg/ml DAPI (Sigma) for 2 min, transferred to poly-L-lysine (Sigma)-covered 35-mm glass-bottomed dishes (MatTek Corporation) in PBS, and imaged using a Zeiss LSM 880 confocal microscope (Zeiss).

Xenopus Oocyte Assays

cDNAs for *Drosophila* AQPs (Drip, Prip, Eglp2, Eglp4), human AQP4 and mefugu AQP8 were cloned into pGEMHE, a plasmid optimized for cRNA expression in *Xenopus laevis* oocytes. cRNA synthesis, oocyte injections (10 ng/oocyte) and oocyte care were performed as previously (58). To ensure basic water channel-activity before detailed analysis, oocytes expressing AQPs were placed in distilled water and time for swelling and ultimately bursting noted.

To calculate permeability to water (osmotic), glycerol, mannitol and urea, we used a Zeiss Lumar, ZEN 2.0 and a four well-perfusion chamber (1-1.5 ml) and acquired images every 5 s for 10 min. For osmotic water permeability, we diluted ND96 (200 mOsm) to 70 mOsm. Permeability for

glycerol, mannitol and urea, were assessed by exposing oocytes to 200 mM solute (2 mM HEPES, pH 7.5) from ND96. Solutions were perfused into the chamber (full solution change in 20 s) beginning at 45-50 seconds into the experiment. To prevent contamination effects, i.e., not returning to baseline volume, oocytes were only exposed to one osmotic or solute challenge. The experiments were repeated for each of the different substrates, and oocytes from at least three different donor *Xenopus* were used.

Water permeability (P_f) was calculated as before (59, 60):

$$P_f = V_0 \left[d\left(\frac{V}{V_0}\right) dt \right] / [(S)(\Delta Osm)(V_w)] \quad \textbf{(Eq. 1)}$$

Data analysis:

Experiments were analyzed using a custom macro in FIJI. The image files were first converted to an 8-bit image then made binary. The analyze particles function was used to measure the major (a) and minor (b) diameter of all four oocytes (3µm per pixel). The 3rd axis (c) for ellipsoid volume was calculated as the average of the major and minor axes. Ellipsoid surface area is calculated as:

$$SA_{ellipsoid} = 4\pi * \sqrt[p]{\left[\frac{a^p b^p + a^p c^p + b^p c^p}{3}\right]} \quad \textbf{(Eq. 2)}$$

where p ≈ 1.6075. This $SA_{ellipsoid}$ is then multiplied by 8 to account for the SA convolutions of the oocyte. Finally, Permeability of solute (P_{solute}) is calculated:

$$P_{solute}\ (cm/s) = \Delta(SA_{ellipsoid}/V_{ellipsoid})/\Delta t \quad \textbf{(Eq. 3)}$$

where Δt= each 20 s (4 point) interval after solute addition. P_{solute} (cm/s) was maximal by 120s after change to 200 mM solute. We then used a 4 point rolling average 120 s after the test solute as the reported value P_{solute} (cm/s) for each oocyte. Number of injected oocytes used for each experiment are presented in **Table S2**.

Desiccation Stress Assay

7-day old male and female flies of specified genotype were anaesthetised briefly with CO_2 and placed in groups of 30 in empty vials (no food or water), and the open end of the tube was sealed with parafilm (Bemis, NA, USA). Flies were counted until 100% mortality was reached and data expressed as % survival ± SEM (n = 3).

Statistical Analysis

GraphPad Prism 7.0 software (GraphPad Software Inc., CA, USA) was used for statistical analysis and generation of graphs. For fluid secretion analysis, a two-tailed Student's *t*-test, taking $P = 0.05$ as the critical value (for two independent groups: basal versus stimulated), was used. For mRNA level quantification, one-way analysis of variance (ANOVA) followed by Tukey's multiple comparisons of means with a significance level of $P < 0.05$ (for three independent groups) was used. For

measurement of oocyte water and solutes permeability, we used an ANOVA analysis for each group with a significance level of $P < 0.05$. For survival curves obtained in desiccation assays, significance was assessed by the log-rank (Mantel-Cox) test. Log-rank tests were conducted for each pairwise comparison.

Acknowledgments

We thank Vilija Lomeikaite, Keith Graham and Leonardo Beltránfor experimental assistance. Fly lines were obtained from the VDRC RNAi stocks (Vienna Drosophila Resource Center, Austria), Bloomington Stock Center (Indiana University, Bloomington, USA) and Fly Stocks of National Institute of Genetics (Japan). This work was funded by the Biotechnology and Biological Sciences Research Council (UK) grants BB/L002647/1 (SD/JATD/ST) and BB/P008097/1 (SD/JATD/ST) and National Institutes of Health Grants DK100227, DK101405 (MFR).

References

1. S. H. P. Maddrell, The fastest fluid-secreting cell known: the upper Malpighian tubule cell of *Rhodnius*. *BioEssays* **13**, 357-362 (1991).
2. J. A. T. Dow *et al.*, The Malpighian tubules of *Drosophila melanogaster:* a novel phenotype for studies of fluid secretion and its control. *J. exp. Biol.* **197**, 421- 428 (1994).
3. M. A. Sözen, J. D. Armstrong, M. Y. Yang, K. Kaiser, J. A. T. Dow, Functional domains are specified to single-cell resolution in a *Drosophila* epithelium. *Proceedings of the National Academy of Sciences of the United States of America* **94**, 5207-5212 (1997).
4. K. W. Beyenbach, H. Skaer, J. A. T. Dow, The developmental, molecular, and transport biology of Malpighian tubules. *Annual Review of Entomology* **55**, 351-374 (2010).
5. B. Denholm *et al.*, Dual origin of the renal tubules in *Drosophila*: mesodermal cells integrate and polarize to establish secretory function. *Curr Biol* **13**, 1052-1057 (2003).
6. S. A. Davies *et al.*, Analysis and inactivation of vha55, the gene encoding the vacuolar ATPase B-subunit in Drosophila melanogaster reveals a larval lethal phenotype. *J Biol Chem* **271**, 30677-30684 (1996).
7. J. P. Day *et al.*, Identification of two partners from the bacterial Kef exchanger family for the apical plasma membrane V-ATPase of Metazoa. *Journal of Cell Science* **121**, 2612-2619 (2008).
8. M. J. O'Donnell, S. H. P. Maddrell, Fluid reabsorption and ion transport by the lower Malpighian tubules of adult female *Drosophila*. *J. exp. Biol.* **198**, 1647-1653 (1995).
9. L. S. Torrie *et al.*, Resolution of the insect ouabain paradox. *Proceedings of the National Academy of Sciences of the United States of America* **101**, 13689-13693 (2004).
10. J. M. Evans, A. K. Allan, S. A. Davies, J. A. T. Dow, Sulphonylurea sensitivity and enriched expression implicate inward rectifier K^+ channels in *Drosophila melanogaster* renal function. *J. exp.Biol.* **208**, 3771-3783 (2005).
11. Y. Wu, M. Baum, C. L. Huang, A. R. Rodan, Two inwardly rectifying potassium channels, Irk1 and Irk2, play redundant roles in Drosophila renal tubule function. *Am J Physiol Regul Integr Comp Physiol* **309**, R747-756 (2015).
12. C. M. Sciortino, L. D. Shrode, B. R. Fletcher, P. J. Harte, M. F. Romero, Localization of endogenous and recombinant Na^+-driven anion exchanger protein NDAE1 from *Drosophila melanogaster*. *Am J Physiol Cell Physiol* **281**, C449-463. (2001).
13. S. M. Linton, M. J. O'Donnell, Contributions of K^+:Cl^- cotransport and Na^+/K^+-ATPase to basolateral ion transport in Malpighian tubules of *Drosophila melanogaster*. *J. exp.Biol.* **202**, 1561-1570 (1999).

14. A. R. Rodan, M. Baum, C. L. Huang, The Drosophila NKCC Ncc69 is required for normal renal tubule function. *Am J Physiol Cell Physiol* **303**, C883-C894 (2012).
15. J. A. T. Dow, The versatile stellate cell - more than just a space-filler. *J Insect Physiol* **58**, 467-472 (2012).
16. B. Denholm *et al.*, The tiptop/teashirt genes regulate cell differentiation and renal physiology in Drosophila. *Development* **140**, 1100-1110 (2013).
17. E. M. Blumenthal, Regulation of chloride permeability by endogenously produced tyramine in the Drosophila Malpighian tubule. *Am J Physiol Cell Physiol* **284**, C718-728 (2003).
18. M. J. O'Donnell, J. A. T. Dow, G. R. Huesmann, N. J. Tublitz, S. H. P. Maddrell, Separate control of anion and cation transport in malpighian tubules of *Drosophila melanogaster*. *Journal of Experimental Biology* **199**, 1163-1175 (1996).
19. S. Terhzaz *et al.*, Isolation and characterization of a leucokinin-like peptide of Drosophila melanogaster. *Journal of Experimental Biology* **202**, 3667-3676 (1999).
20. H. A. MacMillan *et al.*, Anti-diuretic activity of a CAPA neuropeptide can compromise Drosophila chill tolerance. *J Exp Biol* **221** (2018).
21. P. Cabrero *et al.*, Chloride channels in stellate cells are essential for uniquely high secretion rates in neuropeptide-stimulated Drosophila diuresis. *Proc Natl Acad Sci U S A* **111**, 14301-14306 (2014).
22. D. Feingold *et al.*, secCl is a cys-loop ion channel necessary for the chloride conductance that mediates hormone-induced fluid secretion in Drosophila. *Sci Rep* **9**, 7464 (2019).
23. N. Kaufmann *et al.*, Developmental Expression and Biophysical Characterization of a Drosophila melanogaster Aquaporin. *American Journal of Physiology Cell Physiology* **289**, C397-C407 (2005).
24. J. Wang *et al.*, Function-informed transcriptome analysis of *Drosophila* renal tubule. *Genome Biology* **5**, R69 (2004).
25. V. R. Chintapalli, J. Wang, P. Herzyk, S. A. Davies, J. A. T. Dow, Data-mining the FlyAtlas online resource to identify core functional motifs across transporting epithelia. *BMC Genomics* **14**, 518 (2013).
26. K. Liu, H. Tsujimoto, S. J. Cha, P. Agre, J. L. Rasgon, Aquaporin water channel AgAQP1 in the malaria vector mosquito Anopheles gambiae during blood feeding and humidity adaptation. *Proc Natl Acad Sci U S A* **108**, 6062-6066 (2011).
27. P. V. Pietrantonio, C. Jagge, L. L. Keeley, L. S. Ross, Cloning of an aquaporin-like cDNA and in situ hybridization in adults of the mosquito Aedes aegypti (Diptera: Culicidae). *Insect Mol Biol* **9**, 407-418 (2000).
28. L. L. Drake, D. P. Price, S. E. Aguirre, I. A. Hansen, RNAi-mediated gene knockdown and in vivo diuresis assay in adult female Aedes aegypti mosquitoes. *J. Vis. Exp.* 10.3791/3479

3479 [pii], e3479 (2012).
29. L. L. Drake, S. D. Rodriguez, I. A. Hansen, Functional characterization of aquaporins and aquaglyceroporins of the yellow fever mosquito, Aedes aegypti. *Sci Rep* **5**, 7795 (2015).
30. L. Misyura, G. Y. Yerushalmi, A. Donini, A mosquito entomoglyceroporin, Aedes aegypti AQP5, participates in water transport across the Malpighian tubules of larvae. *J Exp Biol* **220**, 3536-3544 (2017).
31. X. X. Yao, Q. W. Meng, G. Q. Li, RNA interference-mediated functional characterization of aquaporin genes in Tribolium castaneum. *Insect Mol Biol* **27**, 234-246 (2018).
32. J. B. Duffy, GAL4 system in Drosophila: a fly geneticist's Swiss army knife. *Genesis* **34**, 1-15 (2002).
33. R. Zardoya, Phylogeny and evolution of the major intrinsic protein family. *Biol Cell* **97**, 397-414 (2005).
34. V. R. Chintapalli, J. Wang, J. A. T. Dow, Using FlyAtlas to identify better *Drosophila* models of human disease. *Nature Genetics* **39**, 715-720 (2007).

35. D. P. Leader, S. A. Krause, A. Pandit, S. A. Davies, J. A. T. Dow, FlyAtlas 2: a new version of the *Drosophila melanogaster* expression atlas with RNA-Seq, miRNA-Seq and sex-specific data. *Nucleic Acids Res* **46**, D809-D815 (2017).
36. E. M. Campbell, A. Ball, S. Hoppler, A. S. Bowman, Invertebrate aquaporins: a review. *J Comp Physiol B* **178**, 935-955 (2008).
37. M. Azuma, T. Nagae, M. Maruyama, N. Kataoka, S. Miyake, Two water-specific aquaporins at the apical and basal plasma membranes of insect epithelia: Molecular basis for water recycling through the cryptonephric rectal complex of lepidopteran larvae. *J. Insect Physiol.* **58**, 523-533 (2012).
38. N. Kataoka, S. Miyake, M. Azuma, Aquaporin and aquaglyceroporin in silkworms, differently expressed in the hindgut and midgut of Bombyx mori. *Insect Mol Biol* **18**, 303-314 (2009).
39. S. Terhzaz *et al.*, Insect capa neuropeptides impact desiccation and cold tolerance. *Proc Natl Acad Sci U S A* **112**, 2882-2887 (2015).
40. K. A. Halberg *et al.*, The cell adhesion molecule Fasciclin2 regulates brush border length and organization in Drosophila renal tubules. *Nat Commun* **7**, 11266 (2016).
41. S. Terhzaz *et al.*, Differential gel electrophoresis and transgenic mitochondrial calcium reporters demonstrate spatiotemporal filtering in calcium control of mitochondria. *J Biol Chem* **281**, 18849-18858 (2006).
42. A. Wessing, D. Eichelberg, "Malpighian tubules, rectal papillae and excretion" in The genetics and biology of *Drosophila,* A. Ashburner, T. R. F. Wright, Eds. (Academic Press, London, 1978), vol. 2c, pp. 1-42.
43. K. W. Beyenbach, Regulation of tight junction permeability with switch-like speed. *Curr Opin Nephrol Hypertens* **12**, 543-550 (2003).
44. K. A. Halberg, S. Terhzaz, P. Cabrero, S. A. Davies, J. A. T. Dow, Tracing the evolutionary origins of insect renal function. *Nat Commun* **6**, 6800 (2015).
45. A. A. Pandit, S. A. Davies, G. Smagghe, J. A. T. Dow, Evolutionary trends of neuropeptide signaling in Beetles - a comparative analysis of Coleopteran transcriptomic and genomic data. *Insect Biochem Mol Biol* S0965-1748(19)30341-8 [pii] 10.1016/j.ibmb.2019.103227, 103227 (2019).
46. L. S. Torrie *et al.*, Resolution of the insect ouabain paradox. *Proceedings of the National Academy of Sciences of the United States of America* **101**, 13689-13693 (2004).
47. J. A. T. Dow, K. A. Halberg, S. Terhzaz, S. A. Davies, "*Drosophila* as a Model for Neuroendocrine Control of Renal Homeostasis" in Model Animals in Neuroendocrinology: From Worm to Mouse to Man, M. Ludwig, G. Levkowitz, Eds. (John Wiley & Sons, 2018), pp. 81-100.
48. G. M. Coast, S. G. Webster, K. M. Schegg, S. S. Tobe, D. A. Schooley, The Drosophila melanogaster homologue of an insect calcitonin-like diuretic peptide stimulates V-ATPase activity in fruit fly Malpighian tubules. *J Exp Biol* **204**, 1795-1804. (2001).
49. P. Cabrero *et al.*, The *Dh* gene of *Drosophila melanogaster* encodes a diuretic peptide that acts through cyclic AMP. *J. exp. Biol.* **205**, 3799-3807 (2002).
50. P. Rosay *et al.*, Cell-type specific calcium signalling in a *Drosophila* epithelium. *Journal of Cell Science* **110 (Pt 15)**, 1683-1692 (1997).
51. J. C. Radford, S. A. Davies, J. A. T. Dow, Systematic G-protein-coupled receptor analysis in Drosophila melanogaster identifies a leucokinin receptor with novel roles. *Journal of Biological Chemistry* **277**, 38810-38817 (2002).
52. P. Cabrero, L. Richmond, M. Nitabach, S. A. Davies, J. A. T. Dow, A biogenic amine and a neuropeptide act identically: tyramine signals through calcium in Drosophila tubule stellate cells. *Proc Biol Sci* **280**, 20122943 (2013).
53. J. C. Radford, S. Terhzaz, P. Cabrero, S. A. Davies, J. A. T. Dow, Functional characterisation of the Anopheles leucokinins and their cognate G-protein coupled receptor. *Journal of Experimental Biology* **207**, 4573-4586 (2004).

54. H. L. Lu, C. Kersch, P. V. Pietrantonio, The kinin receptor is expressed in the Malpighian tubule stellate cells in the mosquito Aedes aegypti (L.): a new model needed to explain ion transport? *Insect Biochemistry & Molecular Biology* **41**, 135-140 (2011).
55. S. Terhzaz *et al.*, Mechanism and function of Drosophila capa GPCR: a desiccation stress-responsive receptor with functional homology to human neuromedinU receptor. *PLoS One* **7**, e29897 (2012).
56. S. Terhzaz *et al.*, Cell-specific inositol 1,4,5 trisphosphate 3-kinase mediates epithelial cell apoptosis in response to oxidative stress in Drosophila. *Cell Signal* **22**, 737-748 (2010).
57. T. Pisitkun, J. D. Hoffert, F. Saeed, M. A. Knepper, NHLBI-AbDesigner: an online tool for design of peptide-directed antibodies. *Am J Physiol Cell Physiol* **302**, C154-164 (2012).
58. N. L. Nakhoul, B. A. Davis, M. F. Romero, W. F. Boron, Effect of expressing the water channel aquaporin-1 on the CO2 permeability of Xenopus oocytes. *Am J Physiol* **274**, C543-548 (1998).
59. L. V. Virkki, C. Franke, P. Somieski, W. F. Boron, Cloning and functional characterization of a novel aquaporin from Xenopus laevis oocytes. *J Biol Chem* **277**, 40610-40616 (2002).
60. R. Musa-Aziz, L. M. Chen, M. F. Pelletier, W. F. Boron, Relative CO2/NH3 selectivities of AQP1, AQP4, AQP5, AmtB, and RhAG. *Proc Natl Acad Sci U S A* **106**, 5406-5411 (2009).

Figures

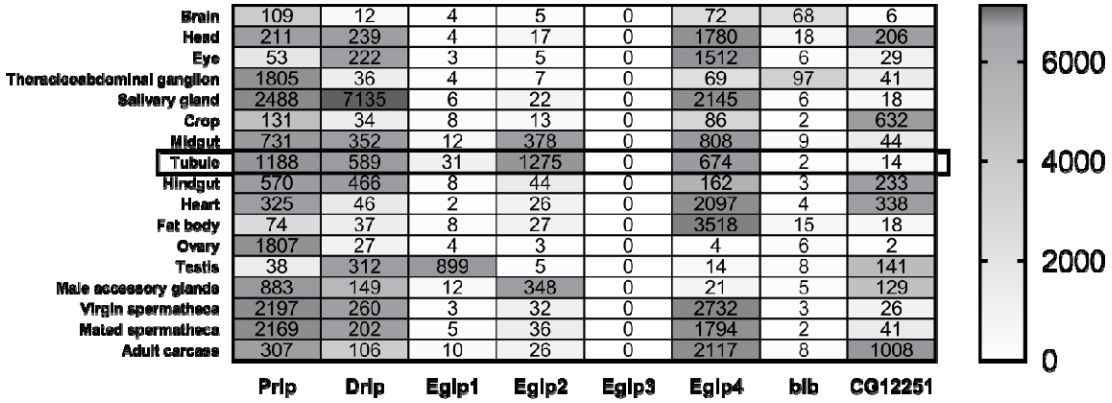

Fig. 1. Major Intrinsic Protein (MIP) family expression in *Drosophila melanogaster*. Data mining of FlyAtlas.org identified four MIP genes (*Prip*, *Drip*, *Eglp2* and *Eglp4*) with highly abundant expression in adult Malpighian tubules.

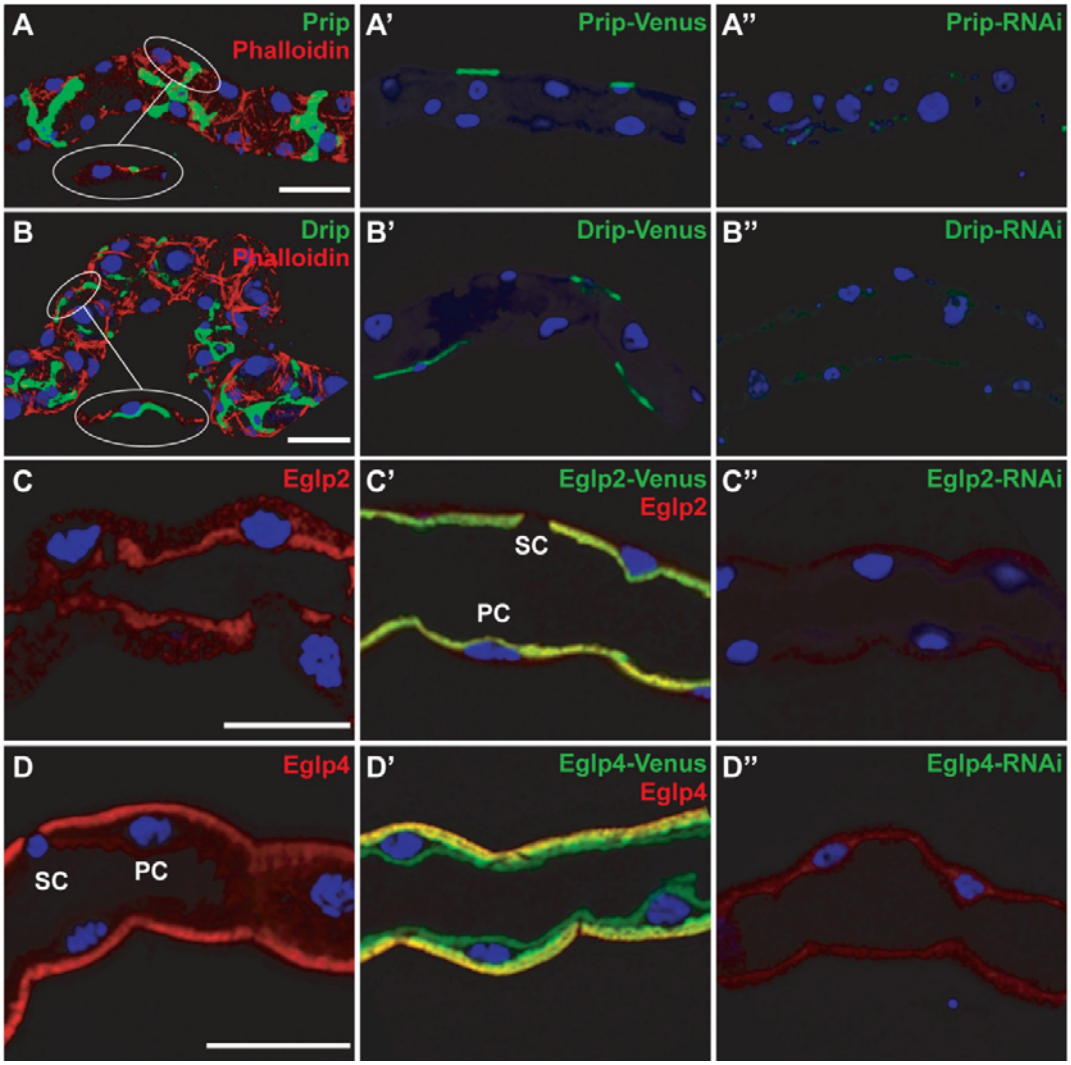

Fig. 2. Subcellular localisation of MIPs in the *Drosophila* tubule. (*A*, *B*) Prip and Drip localise to opposite plasma membranes of the stellate cell (SC). (*A*) Prip is expressed in basolateral membrane (green) and is in a contact with the outside of the tubule, or hemolymph and (*B*) Drip in apical membrane (green) and faces the lumen of the tubule. DAPI (blue) staining for nuclei and phalloidin (red) staining for actin are shown. Inserts are single focal plane images showing magnifications of selected regions. (*A′*, *B′*) Overexpression of Prip and Drip label with Venus (eYFP) recapitulate the pattern of expression observed by immunocytochemistry. (*C*, *D*) Eglp2 and Eglp4 localise to opposite plasma membranes of the principal cell (PC). (*C*) Eglp2 is expressed in apical membrane (red) and (*D*) Eglp4 in basolateral membrane (red), and DAPI (blue). (*C′*, *D′*) Colocalization (yellow) between (*C′*) Eglp2-Venus and Eglp2 to the apical membrane and (*D′*) between Eglp4-Venus and Eglp4 to the basolateral membrane. (*A′′-D′′*) Down-regulation of MIPs in specific cell types using RNAi reduce protein levels. Scale bar = 40 µm.

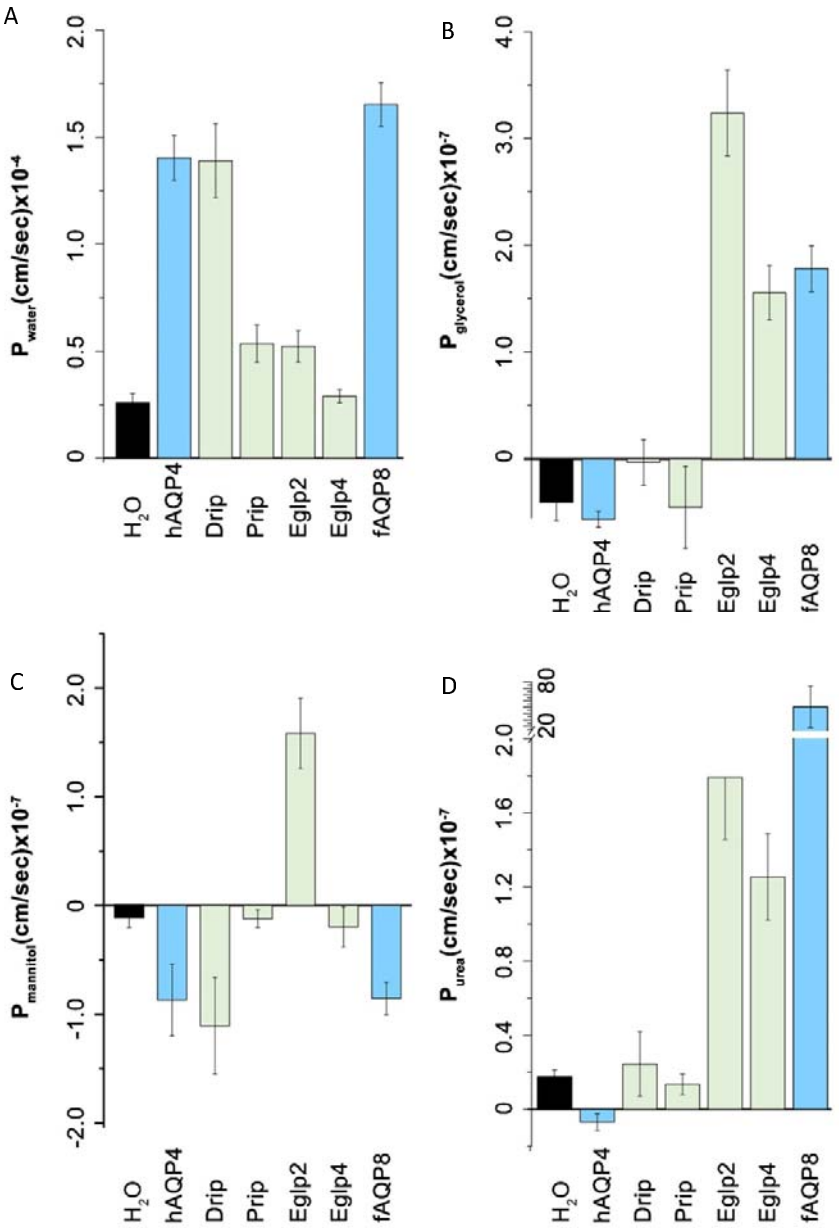

Fig. 3. Transport specificity of *Drosophila* tubule-enriched MIPs. Water-injected control oocytes or oocytes expressing *Drosophila* MIPs (Drip, Prip, Eglp2, Eglp4), human AQP4 (hAQP4) and mefugu AQP8 (fAQP8) were tested for permeability of (A) low osmolarity (Pf, P_{H2O}), (B) urea (P_{urea}), (C) glycerol ($P_{glycerol}$) or (D) mannitol ($P_{mannitol}$).

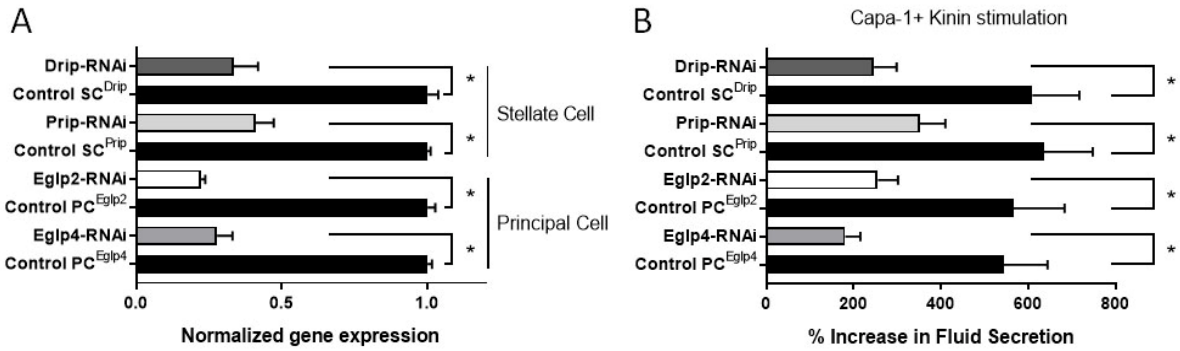

Fig. 4. Validation of MIPs knockdowns and impact of cell-specific down-regulation of MIPs on fluid secretion. (*A*) Effects of knockdowns on tubule mRNA levels for MIPs, validated by qPCR. Cell-specific down-regulation of Eglp2 and Eglp4 in principal cells and Drip and Prip in stellate cells using their respective UAS-dsRNA lines. Data are expressed as mean fold change compared to parental controls ± SEM (n = 3). *P < 0.05 (Student's t-test). (*B*) Impact of cell-specific knockdowns of MIPs on stimulated fluid secretion by tubules in response to Capa-1 and Kinin at 10^{-7} M. Data are expressed as percentage increase from basal fluid secretion compared to parental controls ± SEM (n = 6-10). *P < 0.05 (Student's t-test).

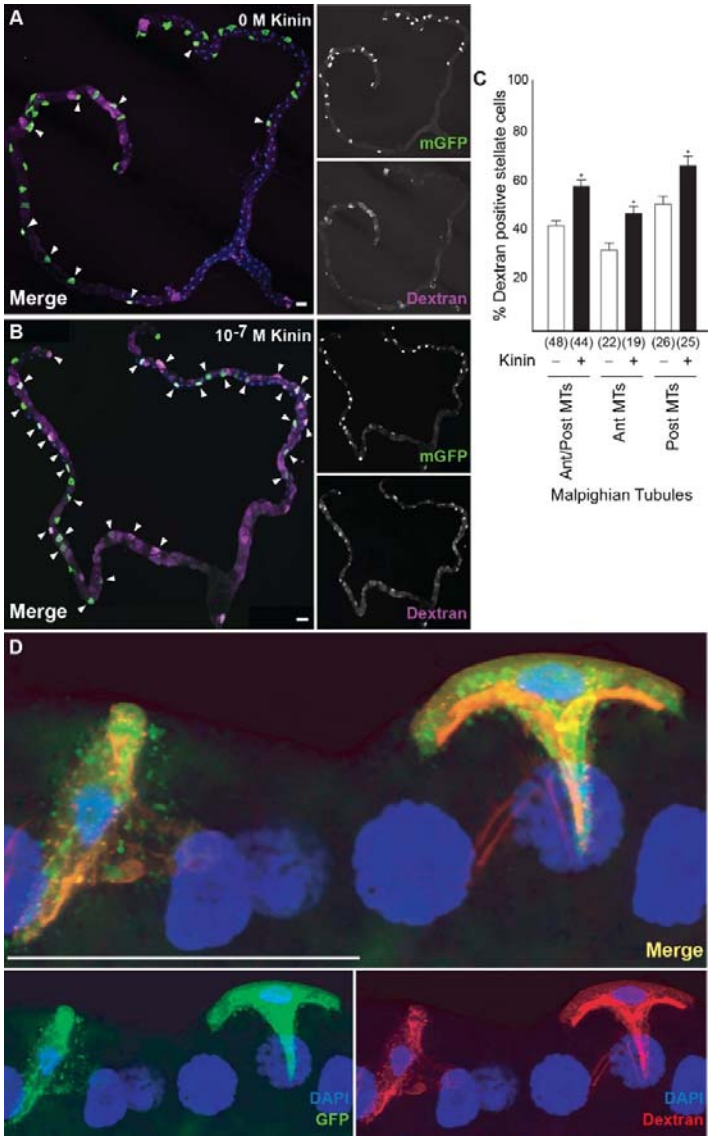

Fig. 5. Dextran labelling demonstrates water flux specifically to the stellate cells. Accumulation of dextran of (*A*) unstimulated and (*B*) following application of Kinin (10^{-7} M) in tubule expressing mGFP in stellate cells. (*C*) Quantification of dextran labelling. Data are expressed as percentage of dextran positive stellate cells in response to 10^{-7} M Kinin compared to unstimulated tubule ± SEM (n = 44-48). *P < 0.05 (Student's t-test). (*D*) Application of 40 kDa dextran conjugated to TRITC dye (red) to tubules in which stellate cells are expressing GFP (green) confirmed the co-localisation of dextran and GFP (yellow); DAPI, blue. Scale bars = 40 µm.

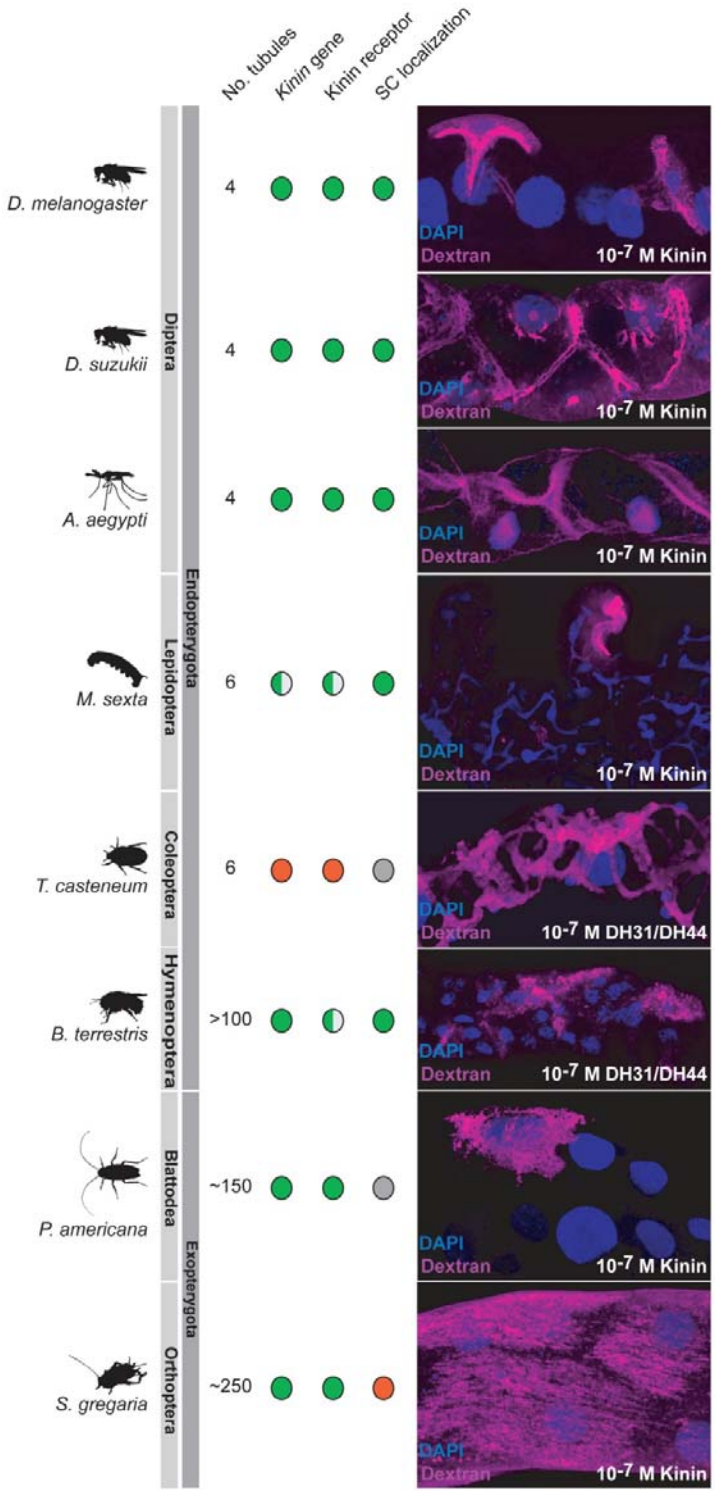

Fig. 6. Dextran labelling is a tool to probe insect biodiversity. The dextran labelling protocol employed for *D. melanogaster* was applied to other insect species, selected from the major insect Orders of exopterygotes and endopterygotes. The distribution of known stellate cells and Kinin labelling (diagnostic of the route of chloride shunt conductance) is reproduced from (44).

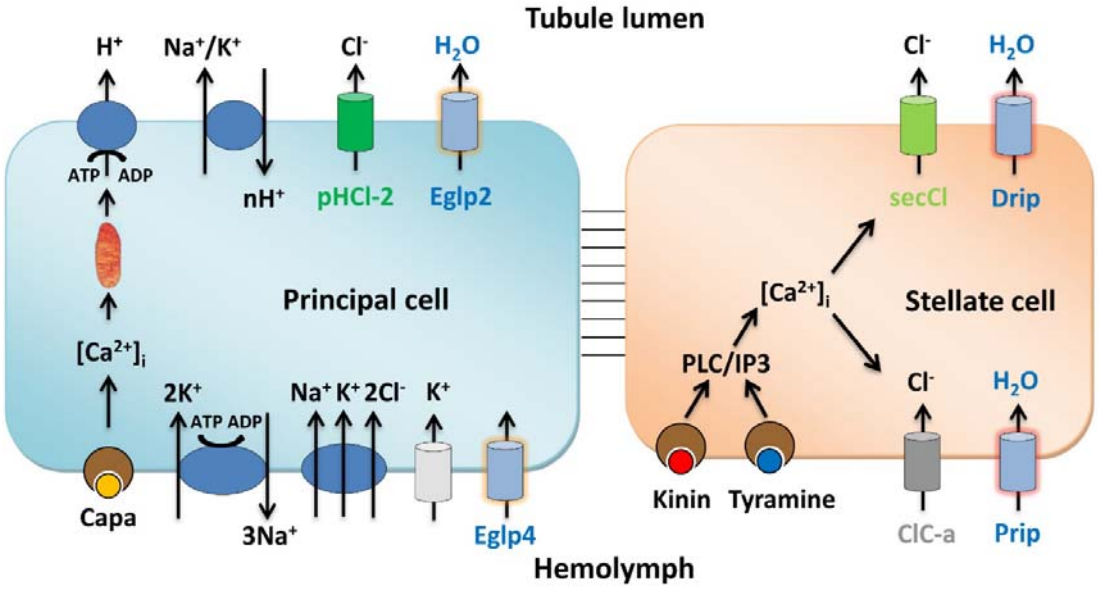

Fig. 7. Model for tubule function. The mitochondria-rich principal cell is specialised for metabolically intensive cation and solute transport. The apical V-ATPase sets up a proton electrochemical gradient which drives net K^+ secretion via NHA or NHE exchangers. Basolateral K^+ entry is afforded by inward-rectifier K^+ channels, Na^+,K^+ ATPase and an Na^+,K^+,$2Cl^-$ cotransport. The resulting lumen positive potential drives a chloride shunt conductance, mainly via basolateral ClC-a and apical secCl channels in the stellate cell. The net transport of KCl drives osmotically obliged water, which is primarily via basolateral Prip and apical Drip in the stellate cells. In this way, the metabolically active principal cell is sheltered from the required high flux rates of water.